

Supporting Information

Mechanical force-induced thermochromic-to-photochromic conversion of a coupled Schiff base hinged via biphenyl moiety
Koichiro Omasa,¹ Isao Yoshikawa,¹ Hirohiko Houjou^{1,2}

¹ Institute of Industrial Science, The University of Tokyo, 4-6-1 Komaba, Meguro-ku, Tokyo 153-8505, Japan.

² Environmental Science Center, The University of Tokyo, 7-3-1 Hongo, Bunkyo-ku, Tokyo 113-0033, Japan.

1. Experimental details (Measurements, Materials, Synthesis)

2. Computational procedure

3. Supplementary figures and table

Figure S1 ¹H NMR (400 MHz, CDCl₃) spectra of compound **bis-SACz**.

Figure S2 ¹³C NMR (100 MHz, CDCl₃) spectra of compound **bis-SACz**.

Figure S3 MALDI-TOF-MS spectra of compound **bis-SACz**.

Figure S4 FT-IR spectra of compound **bis-SACz** in KBr.

Figure S5 Crystal structure of **bis-SACz**.

Figure S6 Crystal structure of **SACz**.

Table S1 Crystallographic data for the **bis-SACz** and **SACz**.

Figure S7 UV-Vis absorption spectra of compounds **bis-SACz** and **SACz** in DCM.

Figure S8 UV-Vis absorption spectra of compound **bis-SACz** in various solvents at specified concentrations.

Figure S9 Absorption spectra of **bis-SACz** in solvents with varied polarity, controlled by the volume ratio of DMSO to DCM.

Table S2 Relative energies (kJ mol⁻¹) of tautomers calculated with solvent effects.

Table S3 TD-DFT characterization of select excited states of **bis-SACz** tautomers.

Figure S10 Isosurface representation for molecular orbitals of **bis-SACz** in enol/enol from (B3LYP/6-311G(d,p)).

Figure S11 Isosurface representation for molecular orbitals of **bis-SACz** in enol/*cis*-keto from (B3LYP/6-311G(d,p)).

Figure S12 Isosurface representation for molecular orbitals of **bis-SACz** in *cis*-keto/*cis*-keto from (B3LYP/6-311G(d,p)).

Figure S13 Calculated absorption spectra of **bis-SACz** tautomers (B3LYP/6-311G(d,p)).

Figure S14 Comparison of absorption spectra (normalized at peak) of **bis-SACz** under various conditions.

Figure S15 Absorption spectra of pristine and ground **SACz** samples.

Figure S16 Definition of geometry parameters for the tautomers of **bis-SACz** and structures optimized by DFT calculation (B3LYP/6-311G** level, in vacuo condition).

Figure S17 Structure of the **bis-SACz** cluster model comprising 19 molecules, and the structures of central molecule in enol/enol, enol/*cis*-keto, *cis*-keto/*cis*-keto forms optimized by ONIOM calculation.

Figure S18 Energy diagram for optimized structures that compares isolation model with cluster model.

Figure S19 Energy diagram for the tautomers that compares the isolation model and cluster model.

Figure S20 Scheme for calculating E_{surr} , ΔE_{conf} and ΔE_{clus} value.

Table S4 Various energies of tautomers derived from the cluster model calculations.

Table S5 Energy values^a (E / kJ mol⁻¹) of **bis-SACz** cluster at each step in the iterative optimization.

Table S6 RMS values of the atomic displacement during iterative optimization of the cluster model calculation.

Figure S21 Energy and RMS values of the cluster model of **bis-SACz** as functions of the iteration step of optimization.

Table S7 Relative energy values between tautomers of **bis-SACz** cluster model.

Figure S22 Relative energy between tautomers of **bis-SACz** cluster model as a function of the iteration step of optimization.

Figure S23 Solid-state ¹³C NMR spectra of pristine and ground **bis-SACz**.

Figure S24 ¹³C NMR (100 MHz, CDCl₃ and DMSO-*d*₆) spectra of **bis-SACz**.

Figure S25 ¹³C NMR (100 MHz, DMSO-*d*₆) spectra of compound **bis-SACz**.

1. Experimental details

Measurements

Solution NMR

^1H and ^{13}C NMR spectra were recorded on a JEOL ECS-400 spectrometer (400 MHz for ^1H) for samples dissolved in deuterated chloroform. The chemical shifts were measured relative to tetramethylsilane (0 ppm), chloroform (77.16 ppm) or dimethyl sulfoxide (39.52 ppm) as an internal standard for ^1H and ^{13}C , respectively.

Solid-state NMR

Solid-state NMR experiments were performed on a JEOL ECA-500 spectrometer operating at a resonance frequency of 125 MHz for ^{13}C . A magic-angle spinning (MAS) probe head (spinning rate: 10 kHz, zirconia rotor of a 4 mm diameter) was used. Each sample (50–60 mg) was packed into the rotor. The $\pi/2$ -pulse duration was 3.6 μs for ^{13}C . Cross-polarization (CP) was performed with a contact time of 1.5 ms, and a relaxation delay of 5 s was applied between scans to ensure adequate relaxation. Chemical shifts for ^{13}C were externally referenced to adamantane, with the methylene peak set at 29.50 ppm. The temperatures were 20.7 °C for the pristine sample and 20.8 °C for the ground sample during the measurements.

Mass spectrometry

Mass spectra were recorded on a JEOL JMS-S3000 MALDI-TOF-MS equipment, for which *trans*-2-[3-(4-tert-Butylphenyl)-2-methyl-2-propenylidene]malononitrile was used as matrix.

Infrared spectroscopy

The IR spectra were measured with a JASCO FT/IR-4X spectrometer.

Ultraviolet-Visible (UV-Vis) Spectroscopy

Solution samples

The ultraviolet-visible (UV-Vis) absorption spectra of the solution samples were measured with a JASCO V-630 spectrophotometer.

Solid samples

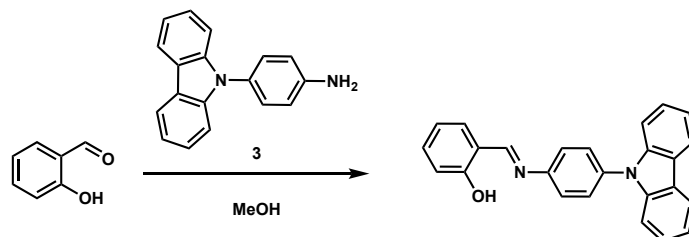
The ultraviolet-visible (UV-Vis) absorption spectra of the solid samples were acquired using a conventional optical microscope equipped with an optical fiber connected to a spectrometer (Ocean Optics USB4000) and a temperature-controlled stage (Linkam THMS600). The incident light was guided from a high-pressure Hg lamp via a 330–380 nm bandpass filter. The samples were prepared by depositing thin-plate crystals obtained by solution recrystallization on a glass slide. The spectra were captured with an acquisition time of 100 ms, and averaged over 10 runs (namely, the total acquisition time of 1.0 s). To capture the spectra of photospecies, the sample was irradiated with an Hg lamp through a dichroic mirror cube, and after the spectral change was saturated the dichroic mirror cube was replaced with a half-mirror cube that intercepts the UV irradiation.

X-ray Diffraction (XRD)

Powder X-ray diffraction (XRD) patterns were obtained on a Rint 2000 diffractometer (Rigaku) using a Cu $K\alpha$ X-ray source (40 kV, 40 mA). The X-ray diffraction data of the single crystals were collected on a Rigaku XtaLAB P200 diffractometer with Cu $K\alpha$ X-rays ($\lambda = 1.54184 \text{ \AA}$). The structures were solved by direct methods (shelxs-2013)¹ and refined on F2 by full-matrix least-squares techniques (shelxl-2018)² using the Yadokari- XG software package.³

Materials

All chemicals and solvents were purchased from Tokyo Kasei Kogyo (TCI) or Kanto Chemical Co., and used without further purification. 4-(9H-carbazol-9-yl) aniline hydrochloride (**3**) and 2-(((4-(9H-carbazol-9-yl)phenyl)imino)methyl)phenol (**SACz**) was prepared according to method previously reported.^{4,5}

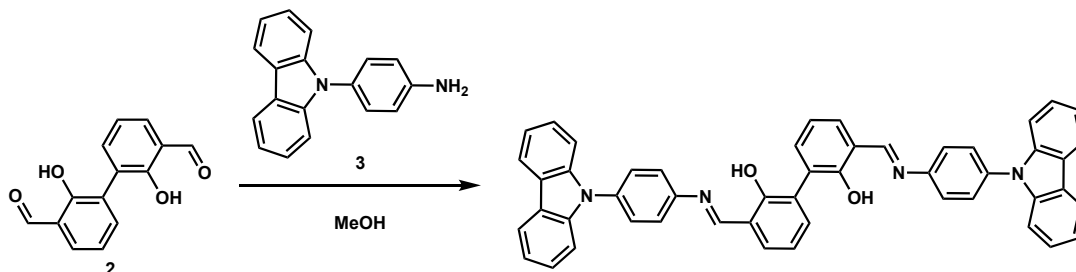


Scheme S1 Synthesis of **SACz**.

4-(9H-carbazol-9-yl) aniline hydrochloride (**3**) (0.4402 g, 1.50 mmol) and NaOH (0.0702 g, 1.76 mmol) were dissolved in dry MeOH (10 mL): solution A. Under nitrogen, Salicylaldehyde (0.32 mL, 3.0 mmol) was added to a solution A with stirring for 1h. The resulting brown solution was concentrated with a rotary evaporator. The solution was extracted with DCM (30 mL \times 3). The combined extract was dried over Na₂SO₄. After removal of the solvent, the residue was purified by recrystallization with hexane/DCM (1:1) to give **SACz** as green crystals (0.8691 g, 2.4mmol, 80 %). ¹H NMR (400 MHz, CDCl₃) δ : 13.17 (s, 1H), 8.76 (s, 1H), 8.16 (d, J = 7.5 Hz, 2H), 7.67-7.62 (m, 2H), 7.55-7.51 (m, 2H), 7.48-7.41 (m, 6H), 7.34-7.29 (m, 2H), 7.08 (d, J = 8.3 Hz, 1H), 7.01 (dt, J = 1.0, 7.3 Hz, 1H) ppm. ¹³C NMR (100 MHz, CDCl₃) δ : 163.17, 161.20, 148.48, 140.81, 136.35, 133.51, 132.48, 128.05, 126.04, 123.45, 122.64, 120.39, 120.10, 119.27, 119.16, 117.38, 109.71 ppm.

Synthesis

2,2'-dihydroxy-[1,1'-biphenyl]-3,3'-dicarbaldehyde (**2**) was prepared according to method previously reported.⁶



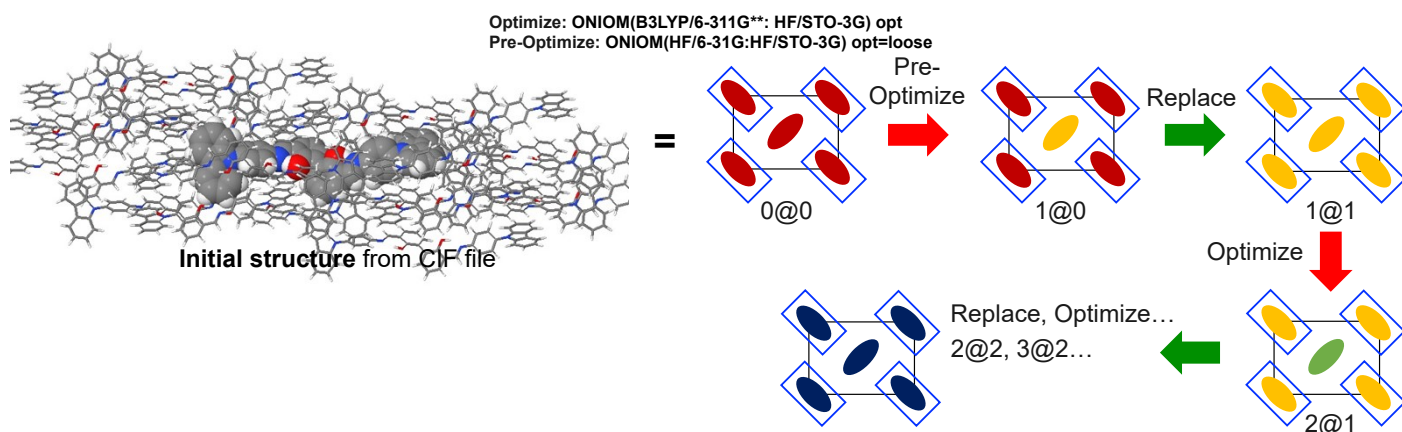
Scheme S1 Synthesis of **bis-SACz**.

2 (0.2577 g, 1.06 mmol) and 4-(9H-carbazol-9-yl) aniline hydrochloride (0.6252 g, 2.12 mmol) were dissolved in dry MeOH (10 mL) with stirring for 1h. The resulting brown solution was concentrated with a rotary evaporator. After removal of the solvent, the residue was washed by ethanol and recrystallized (DCM : Hexane) to give **bis-SACz** as red crystals (0.6820 g, 0.943 mmol, 89 %). m.p. >253.4 °C (decomp.). ¹H NMR (400 MHz, CDCl₃) δ : 13.83 (s, 2H), 8.85 (s, 2H), 8.16 (d, 7.7 Hz, 4H), 7.65-7.61 (m, 4H), 7.59-7.51 (m, 8H), 7.46-7.43 (m, 8H), 7.33-7.29 (m, 4H), 7.13 (t, J = 7.6 Hz, 2H) ppm. ¹³C NMR (100 MHz, CDCl₃) δ : 163.12, 158.92, 147.19, 140.80, 136.42, 135.40, 132.35, 128.07, 126.27, 126.04, 123.45, 122.62, 120.37, 120.10, 119.28, 119.02, 109.74 ppm. IR (KBr): 1617 (ν C=N) cm⁻¹. HRMS(+) m/z 722.2663 (Calc. 722.2682 for M).

2. Computational procedure

For the structural optimization and energy calculations of isolated molecules, Density Functional Theory (DFT) calculations were performed using Gaussian 16. The B3LYP/6-311G** basis set was employed for structural optimization, and the same level of theory was used for single-point energy calculations.

Cluster calculations were also carried out with Gaussian 16, employing the ONIOM method. A 19-molecule cluster was constructed based on space group information obtained from the single crystal, using the CIF file. In these calculations, the central molecule was treated at a high level, while the surrounding molecules were calculated at a low level and set to 'Freeze'. The initial pre-optimization was conducted with ONIOM (HF/6-31G:HF/STO-3G) opt=loose setting, focusing on the central molecule. This optimized central molecule was then reconstituted into a cluster based on the space group, and further optimization was done using ONIOM (B3LYP/6-311G**:^{HF}/STO-3G) opt setting. This optimization process was repeated five times in total. The RMS and energy of each optimization were compared to select the most stable cluster structure. The cluster structure from the third optimization cycle referred to as the 3@3 cluster was selected for its stability. This optimized 3@3 cluster was used for further calculations and is documented alongside the corresponding RMS and energy data in Figures S22 and S23 and Tables S5, S6 and S7. The final energy calculation was performed using a single-point ONIOM (B3LYP/6-311G**:^{HF}/6-31G) QM/QM' calculation.



3. Supplementary figures and table

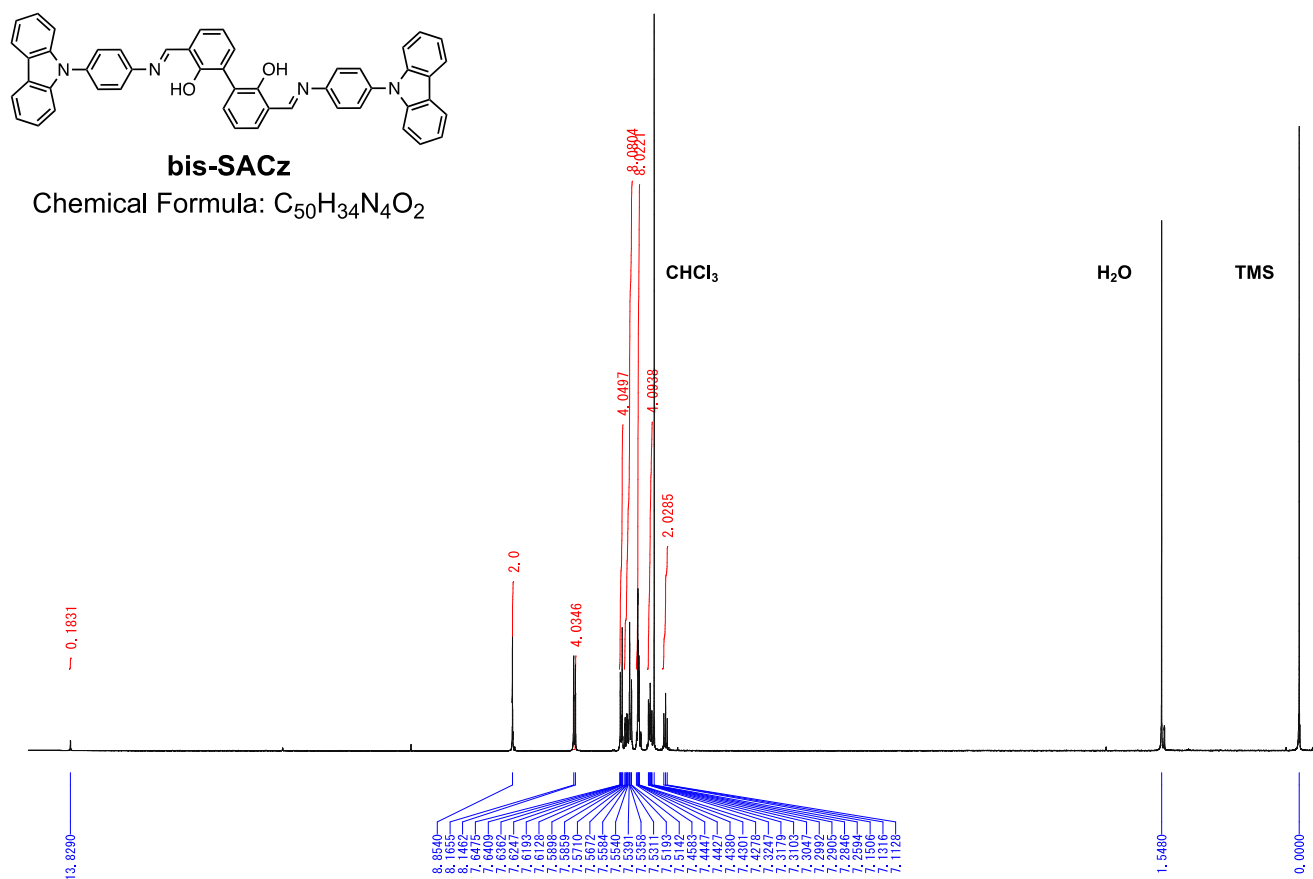


Figure S1 1H NMR (400 MHz, $CDCl_3$) spectra of compound bis-SACz.

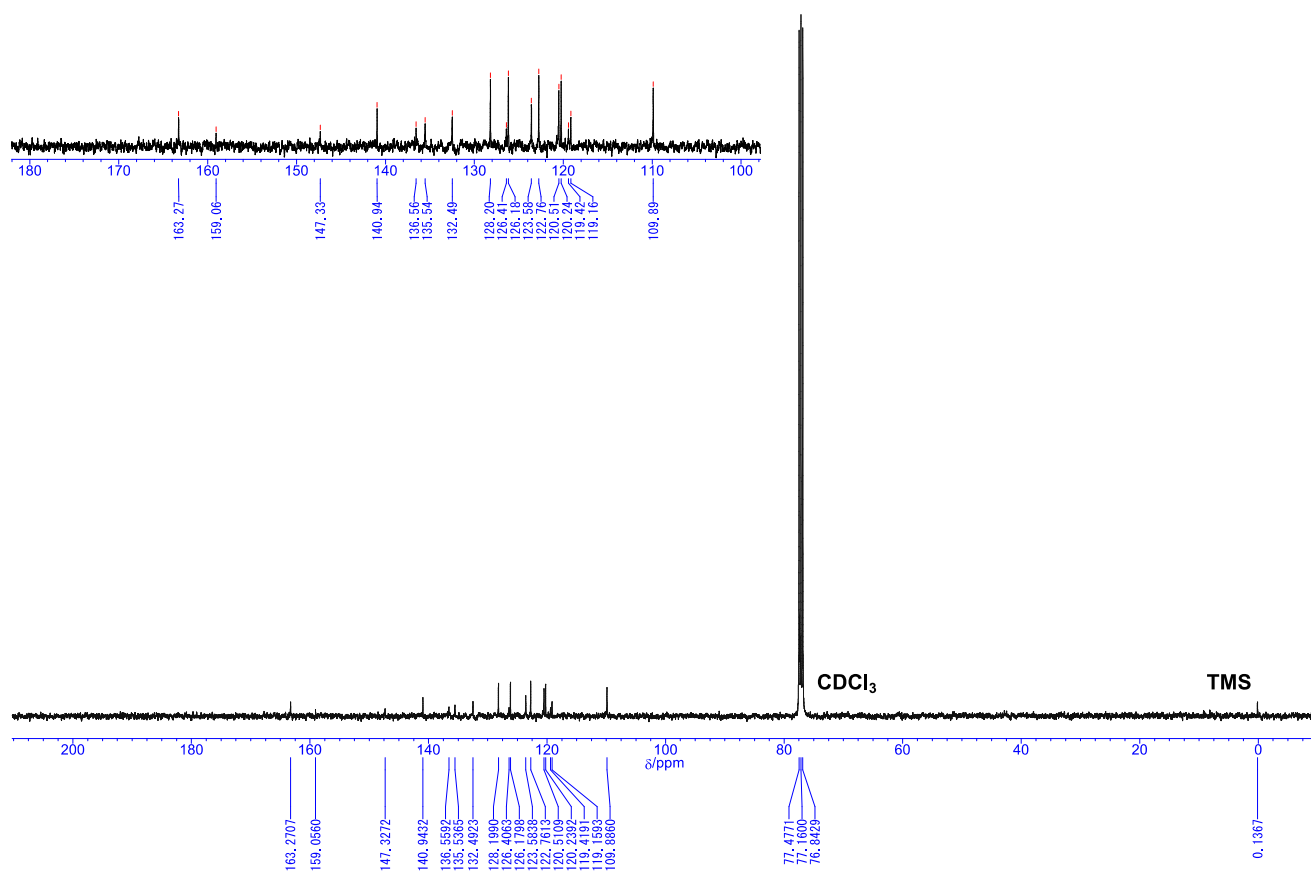


Figure S2 ^{13}C NMR (100 MHz, $CDCl_3$) spectra of compound bis-SACz.

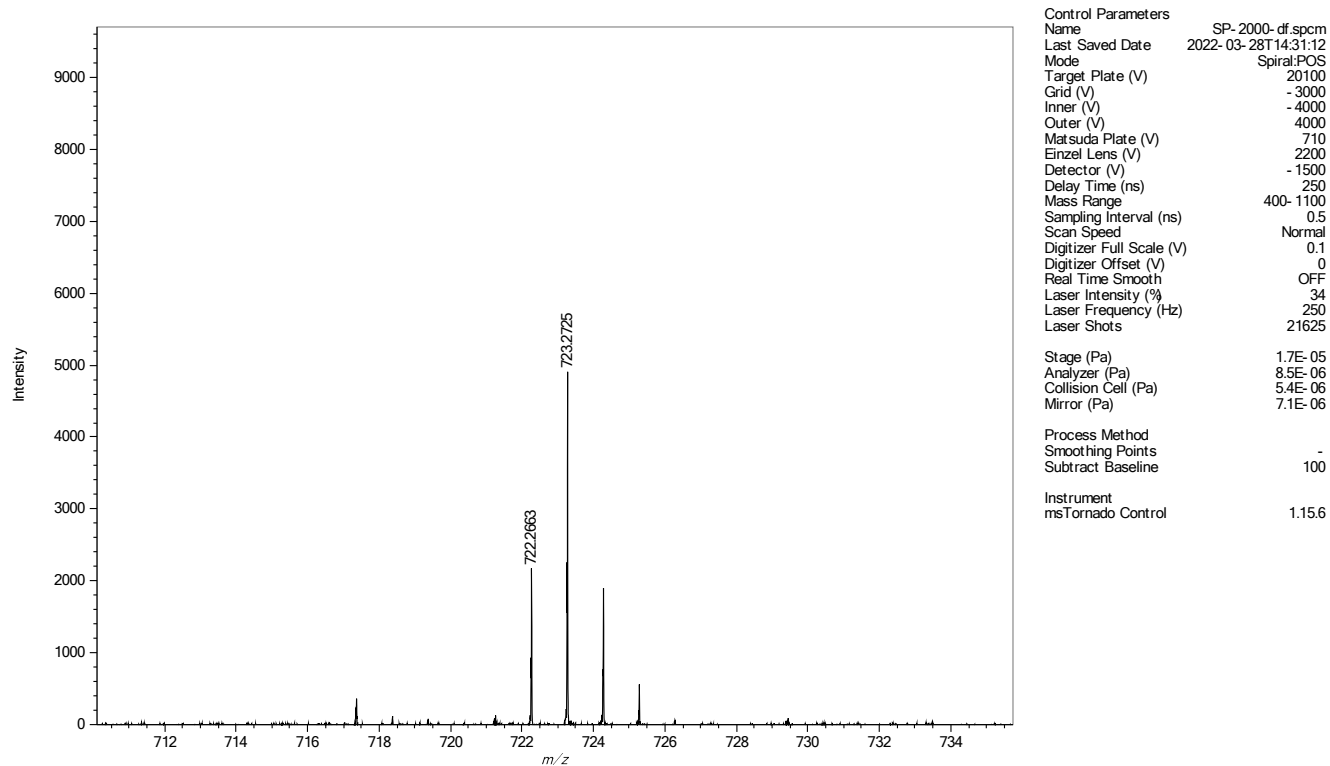


Figure S3 MALDI-TOF-MS spectra of compound **bis-SACz**.

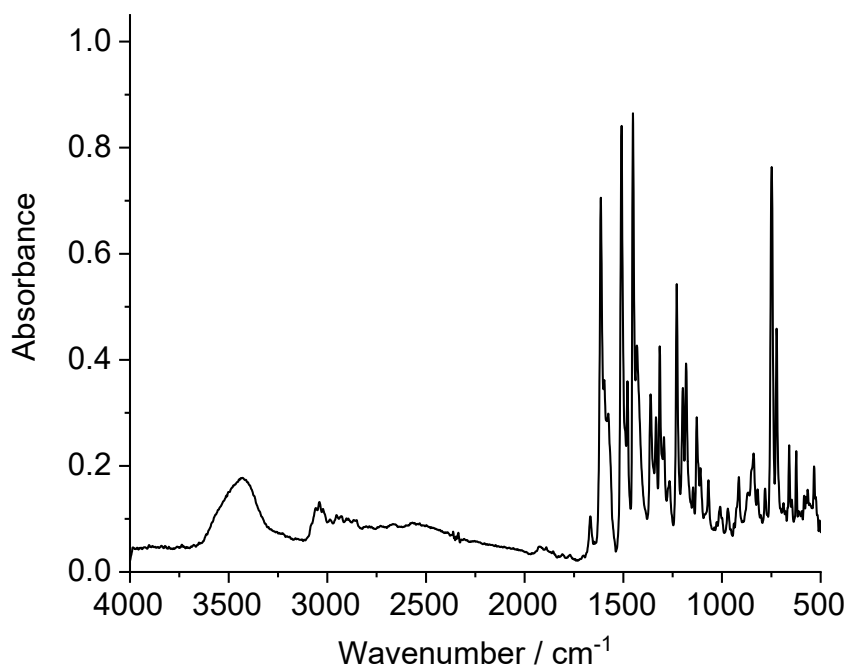


Figure S4 FT-IR spectra of compound **bis-SACz** in KBr.

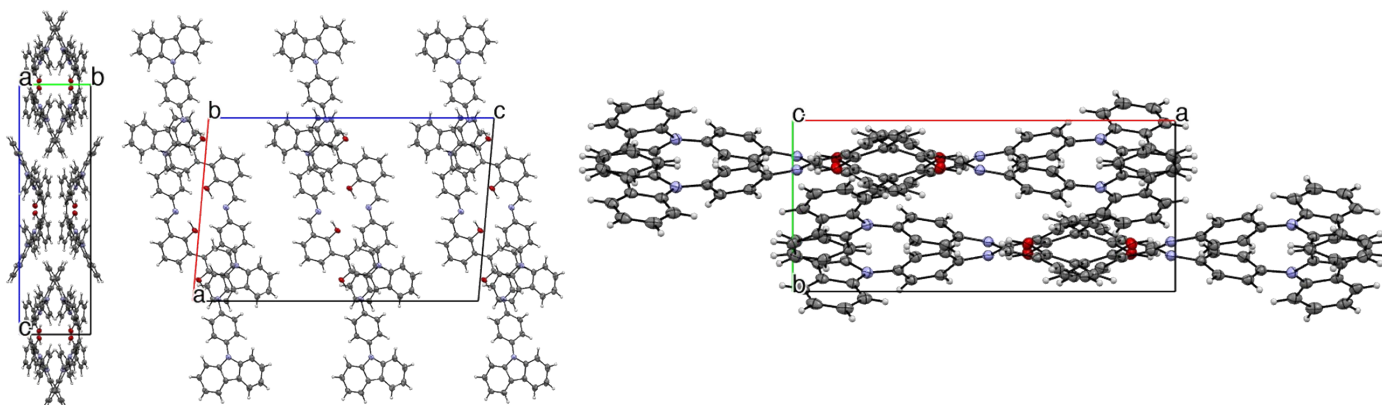


Figure S5 Crystal structure of bis-SACz.

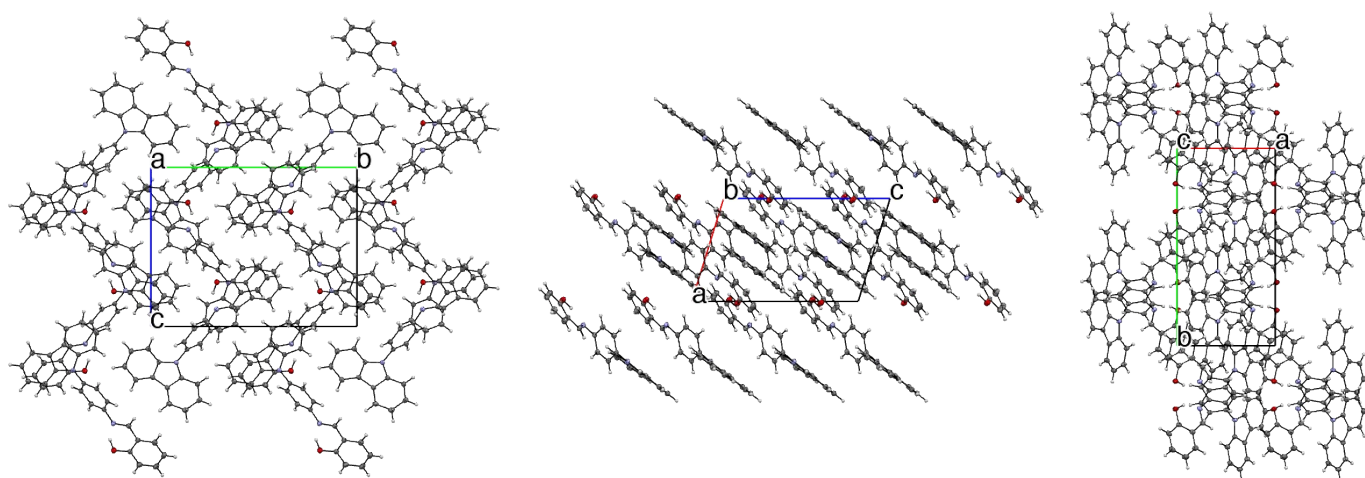


Figure S6 Crystal structure of SACz.

Table S1 Crystallographic data for the **bis-SACz** and **SACz**.

	bis-SACz	SACz
Space group IT number	15	14
Space group	<i>I2/a</i>	<i>P2₁/c</i>
<i>a</i> / Å	17.3879(3)	8.61650(10)
<i>b</i> / Å	7.72700(10)	16.5014(2)
<i>c</i> / Å	27.0872(5)	13.3230(2)
α / °	90	90
β / °	94.9551(16)	107.2274(17)
γ / °	90	90
<i>V</i> / Å ³	3625.73(10)	1809.34(4)
<i>D</i> _{calc} / g cm ⁻³	1.324	1.330
<i>Z</i>	4	4
<i>Z</i>	0.5	1
<i>T</i> / K	93(2)	93(2)
<i>2</i> θ	145.69	145.248
<i>R</i>	0.0379	0.0463
<i>R</i> _w	0.1011	0.1261
<i>R</i> _{int}	0.0350	0.0266
GoFall	1.042	1.082
reflns_number_total	3580	3501
refine_diff_density_max	0.217	0.342
refine_diff_density_min	-0.188	-0.619
crystal description	plate	prism
crystal colour	orange	green

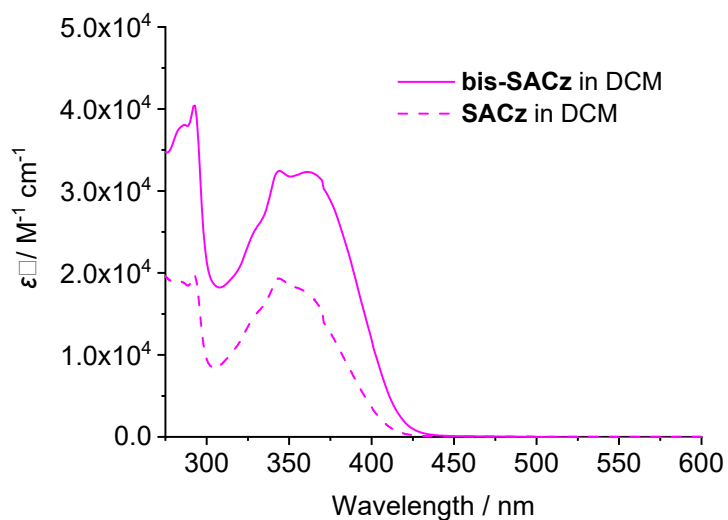


Figure S7 UV-Vis absorption spectra of compounds **bis-SACz** and **SACz** in DCM (1.5×10^{-5} M for **bis-SACz**, 1.1×10^{-5} M for **SACz**).

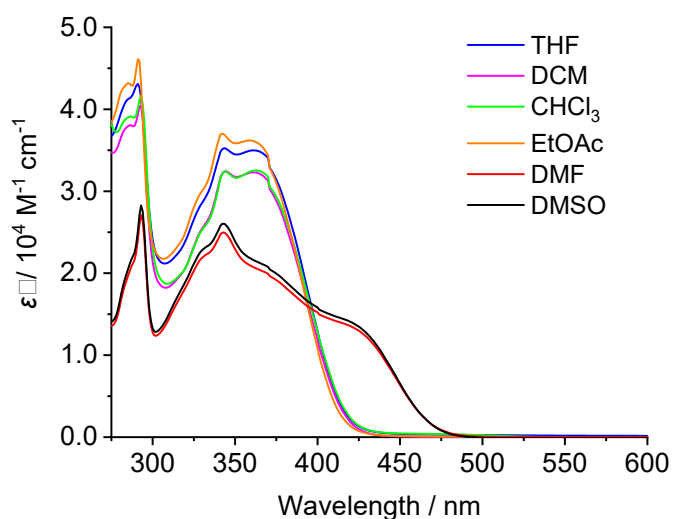


Figure S8 UV-Vis absorption spectra of compound **bis-SACz** in various solvents at specified concentrations: THF (1.4×10^{-5} M), DCM (1.5×10^{-5} M), CHCl_3 (2.4×10^{-5} M), EtOAc (2.2×10^{-5} M), DMF (2.1×10^{-5} M), and DMSO (2.8×10^{-5} M).

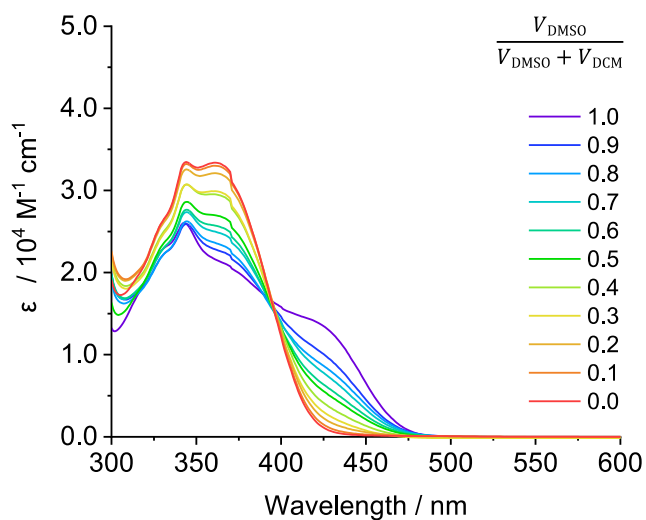


Figure S9 Absorption spectra of **bis-SACz** at 1.5×10^{-5} M in solvents with varied polarity, controlled by the volume ratio of DMSO to DCM ($V_{\text{DMSO}} / (V_{\text{DMSO}} + V_{\text{DCM}})$).

Table S2. Relative energies (kJ mol⁻¹) of tautomers calculated with solvent effects^{a)}

	in vacuo	Chloroform	Tetrahydrofurane	Dichloromethane	Dimethylsulfoxide
enol/enol	(0.0)	(0.0)	(0.0)	(0.0)	(0.0)
enol/ <i>cis</i> -keto	17.2	11.6	10.6	10.4	9.1
<i>cis</i> -keto/ <i>cis</i> -keto	34.5	23.8	22.0	21.4	18.9

a) B3LYP/6-311G(d,p) under polarizable continuum model approximation

Table S3 TD-DFT^{a)} characterization of select excited states of **bis-SACz** tautomers: excitation energy, oscillator strength, and contributions of excitation configurations based on molecular orbital representation.

Tautomers	Assignment	Excitation energy from S ₀ state		Oscillator strength	Excitation configuration	CI coefficient
		Energy / eV	Wavelength / nm			
enol/enol	S ₁	3.0364	408.33	0.6668	HOMO → LUMO	0.4424
					HOMO -1 → LUMO +1	0.3308
					HOMO → LUMO +1	0.2914
					HOMO -1 → LUMO	-0.2953
	S ₂	3.0826	402.20	0.0724	HOMO -1 → LUMO	0.4721
					HOMO → LUMO +1	0.3793
					HOMO → LUMO	0.2548
	S ₅	3.3349	371.78	0.1151	HOMO -3 → LUMO	0.6311
					HOMO → LUMO	0.2108
	S ₁₁	3.7599	329.76	0.0897	HOMO -5 → LUMO	0.6525
	S ₁₂	3.7638	329.41	0.4528	HOMO -5 → LUMO +1	0.6590
					HOMO -5 → LUMO	0.1999
enol/ <i>cis</i> -keto	S ₁	2.6137	474.36	0.5097	HOMO → LUMO	0.6923
	S ₃	2.9323	422.82	0.1172	HOMO -2 → LUMO	0.6470
					HOMO -1 → LUMO	-0.2485
	S ₅	3.1490	393.73	0.3084	HOMO -1 → LUMO +1	0.6730
					HOMO -5 → LUMO	0.1549
	S ₁₂	3.6892	336.07	0.4979	HOMO -6 → LUMO	0.5400
					HOMO -5 → LUMO +1	-0.3433
					HOMO -2 → LUMO +1	-0.2279
<i>cis</i> -keto/ <i>cis</i> -keto	S ₁	2.3429	529.20	0.4940	HOMO → LUMO	0.7055
	S ₄	2.9281	423.43	0.6911	HOMO -1 → LUMO +1	0.5895
					HOMO -2 → LUMO	-0.3722
	S ₁₀	3.3498	370.12	0.1386	HOMO -3 → LUMO +1	0.6296
	S ₁₅	3.7000	335.10	0.5480	HOMO -6 → LUMO	0.5693
HOMO -1 → LUMO +4					-0.3446	
				HOMO -7 → LUMO +1	0.1472	

a) B3LYP/6-311G(d,p)

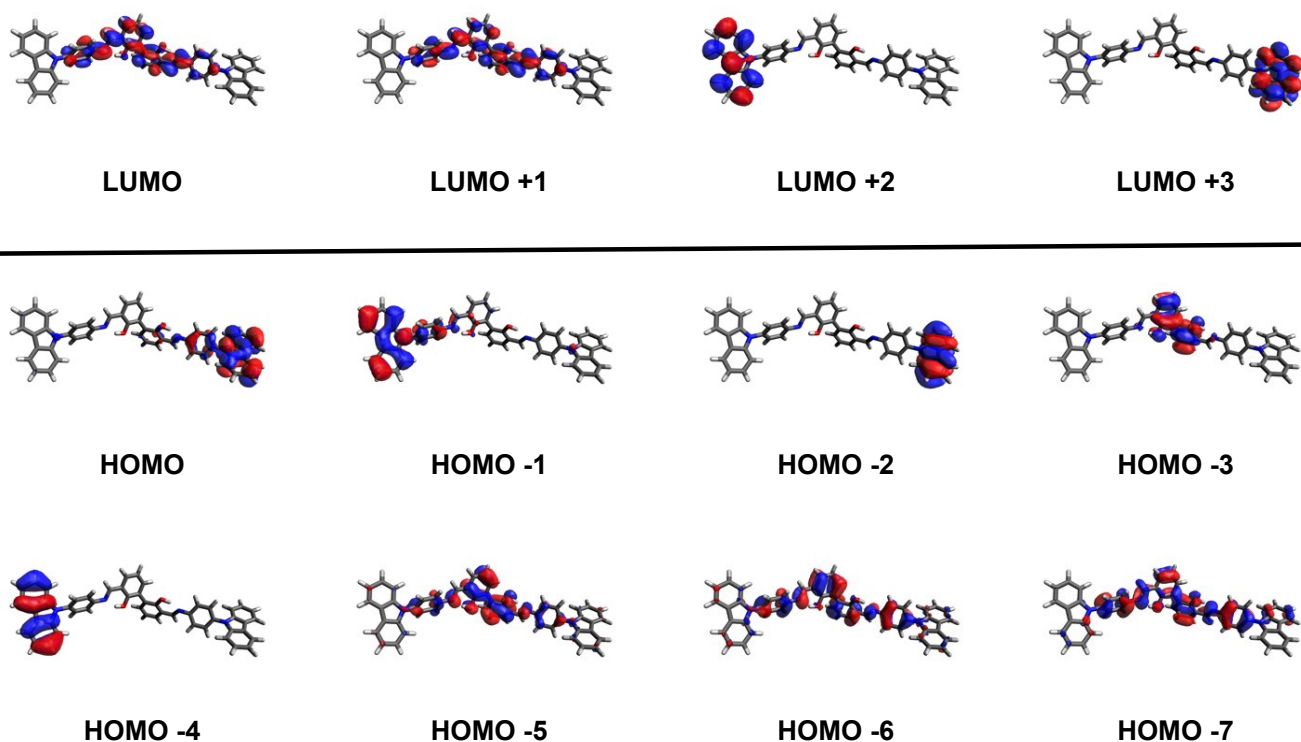


Figure S10 Isosurface representation for molecular orbitals of **bis-SACz** in enol/enol from (B3LYP/6-311G(d,p)).

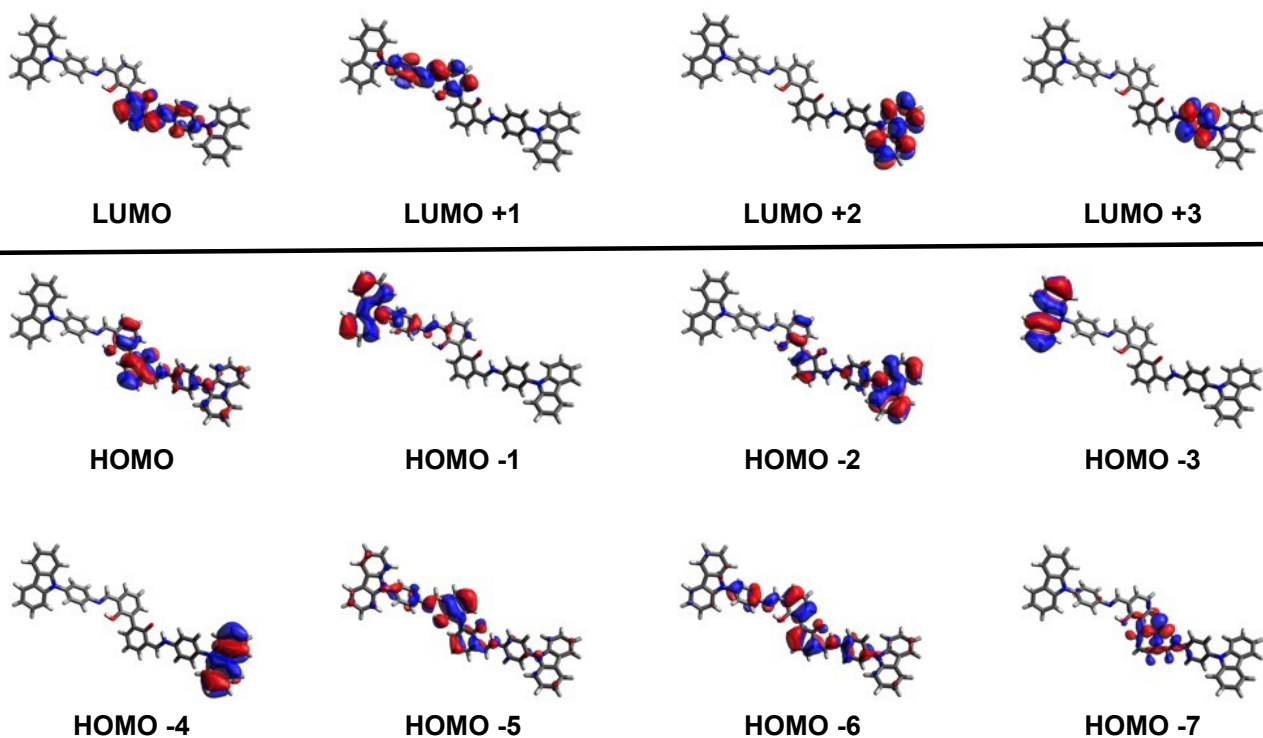


Figure S11 Isosurface representation for molecular orbitals of **bis-SACz** in enol/*cis*-keto from (B3LYP/6-311G(d,p)).

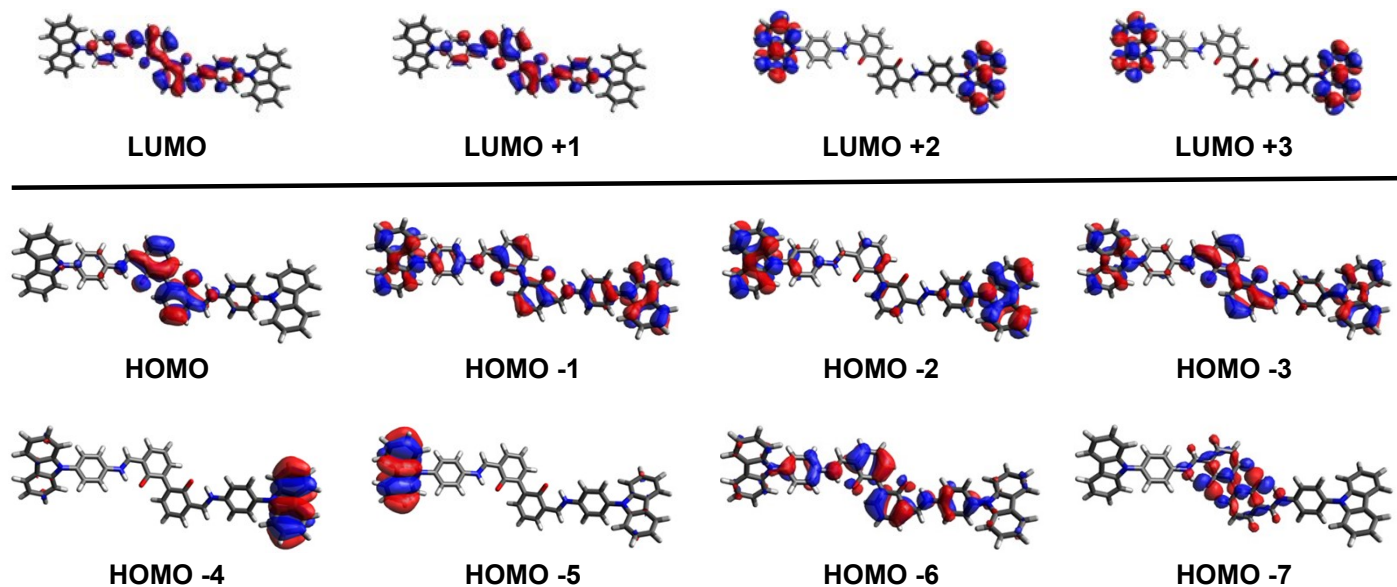


Figure S12 Isosurface representation for molecular orbitals of **bis-SACz** in *cis-keto / cis-keto* from (B3LYP/6-311G(d,p)).

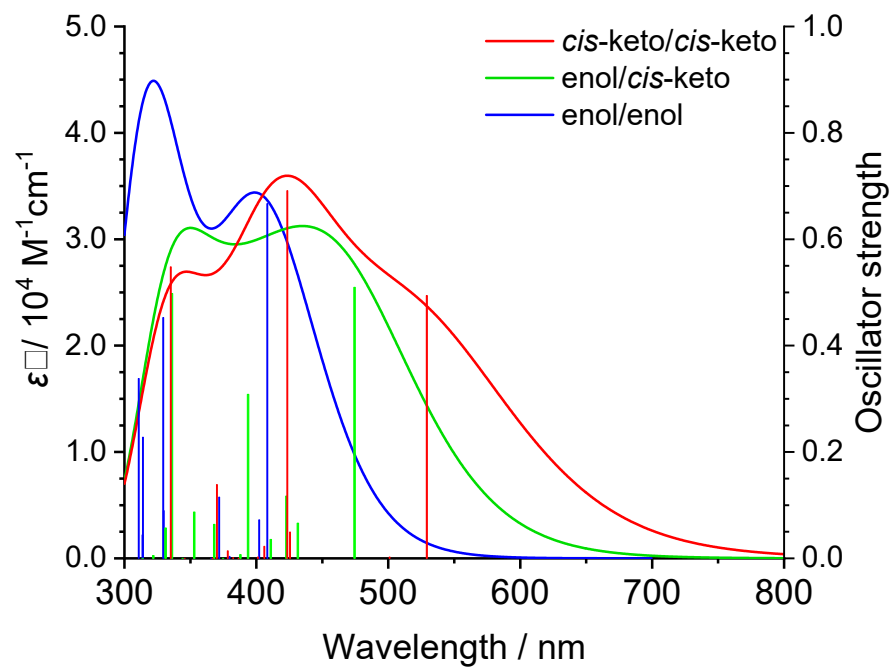


Figure S13 Calculated absorption spectra of **bis-SACz** tautomers (B3LYP/6-311G(d,p)).

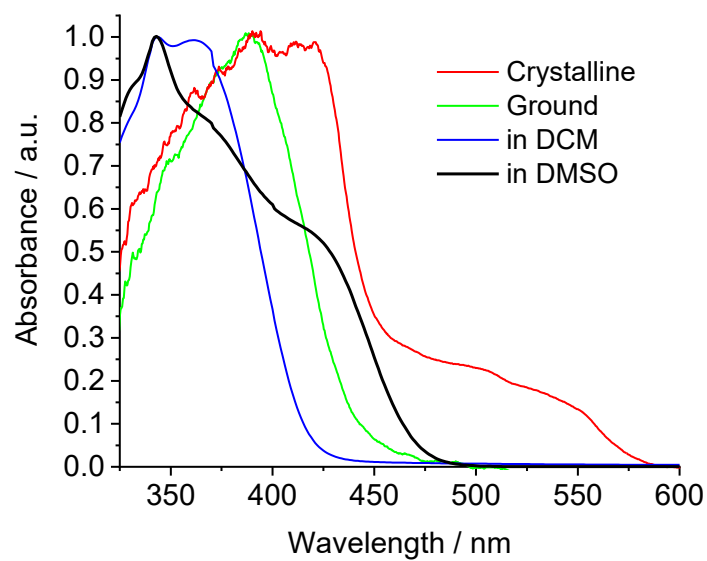


Figure S14 Comparison of absorption spectra (normalized at peak) of **bis-SACz** under various conditions: crystalline state, ground state, DCM solution and DMSO solution.

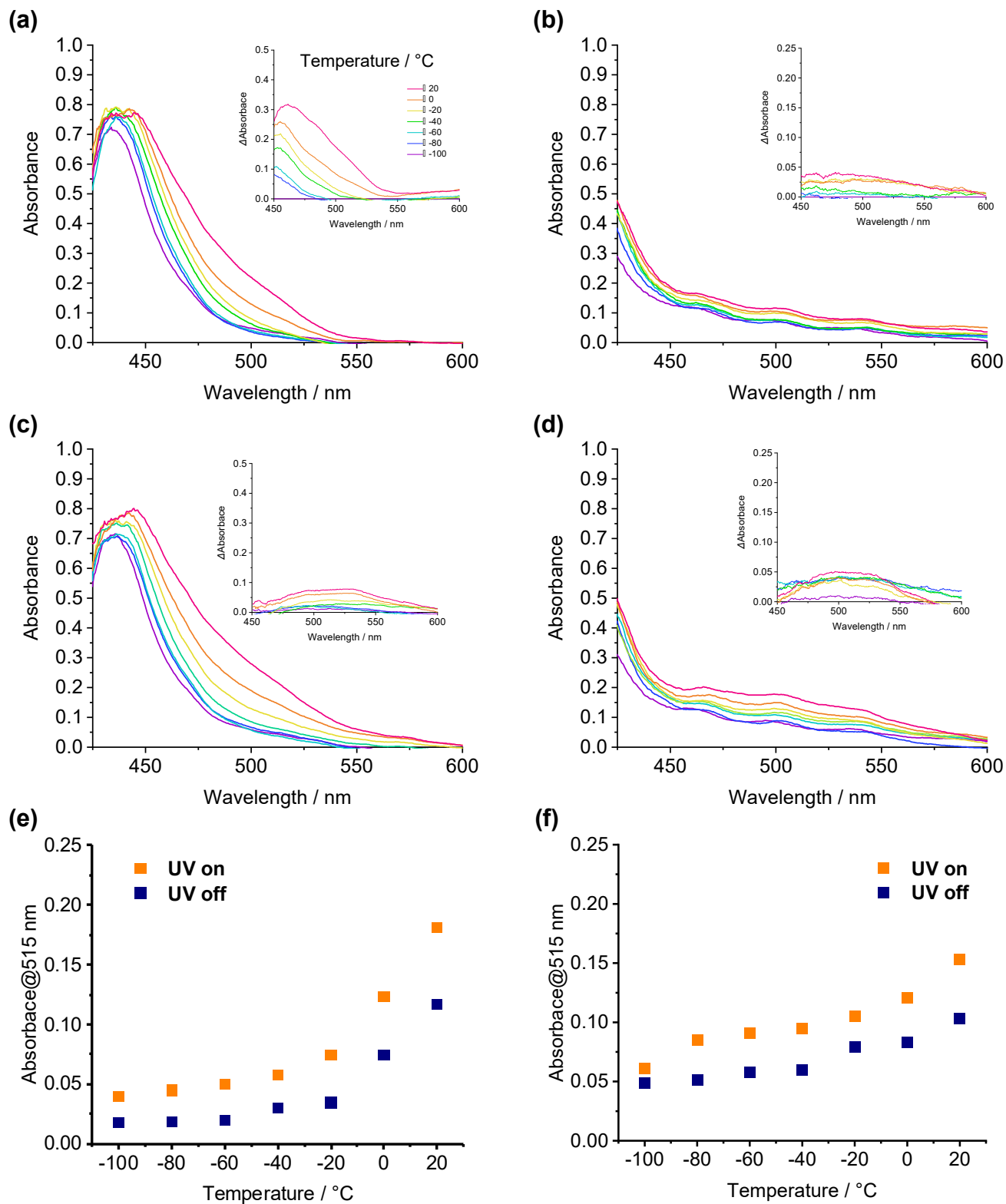


Figure S15 Absorption spectra of (a, c) pristine and (b, d) ground SACz samples measured (a, b) without and (c, d) under UV irradiation. (e, f) Change in absorbance monitored at 515 nm in the dark-adapted and photo-stationary states for crystalline and ground samples, respectively.

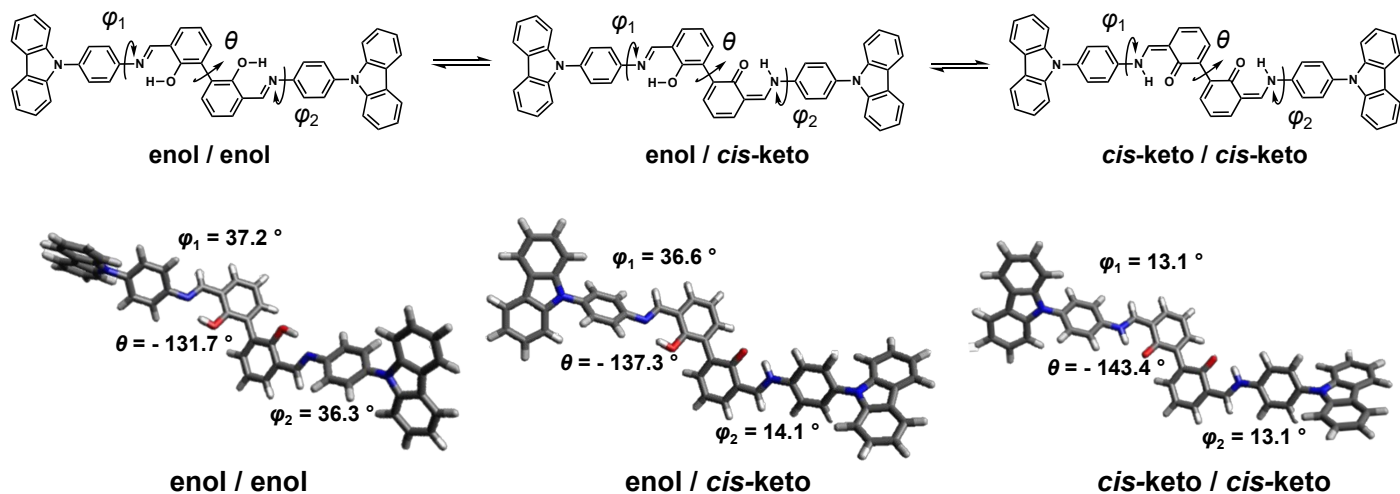


Figure S16 (top) Definition of geometry parameters for the tautomers of **bis-SACz**. (bottom) Structures optimized by DFT calculation (B3LYP/6-311G** level, in vacuo condition) with their geometry parameters denoted.

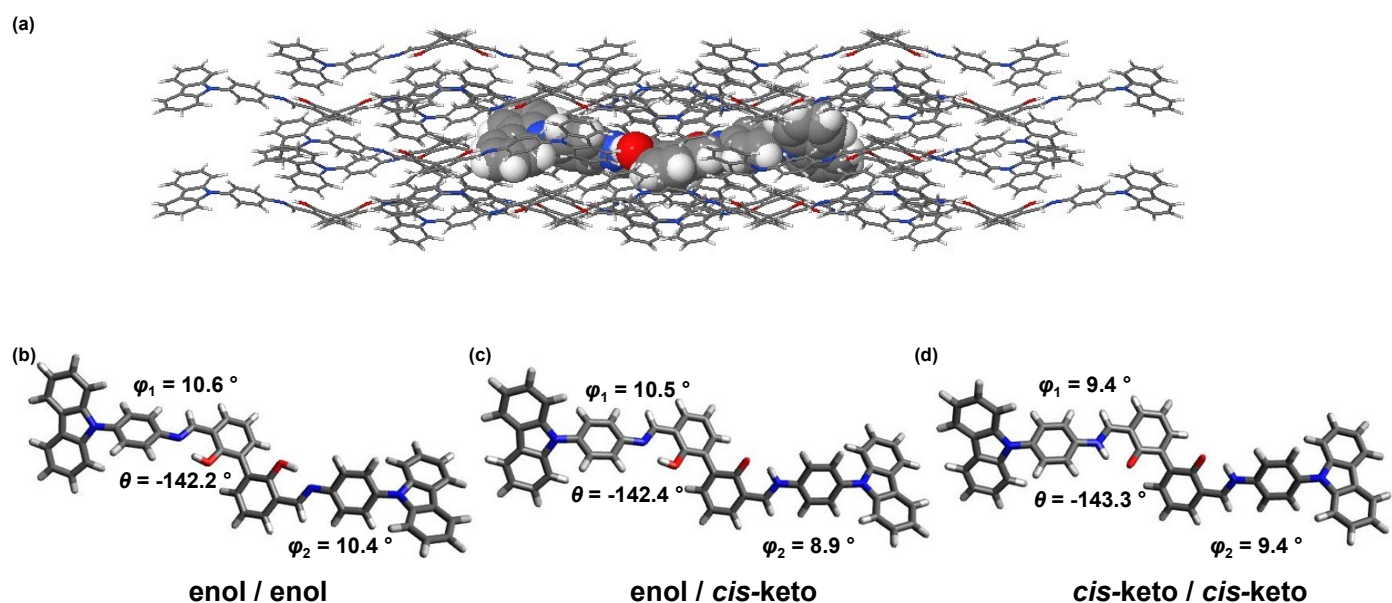


Figure S17 (a) Structure of the **bis-SACz** cluster model comprising 19 molecules, and the structures of central molecule in (b) enol/enol, (c) enol/cis-keto, (d) cis-keto/cis-keto forms optimized by ONIOM calculation (B3LYP/6-311G**: $\text{HF}/6\text{-}31\text{G}$ level, considering molecular surroundings in the cluster) with their geometry parameters denoted.

Isolate : B3LYP/6-311G**

Cluster : ONIOM(B3LYP/6-311G**::HF/6-31G)

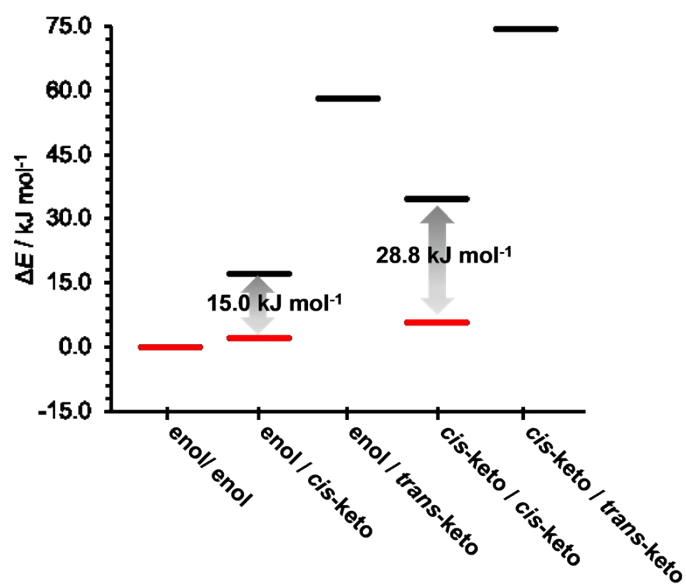


Figure S18 Energy diagram for optimized structures that compares isolation model (black bars) with cluster model (red bars).

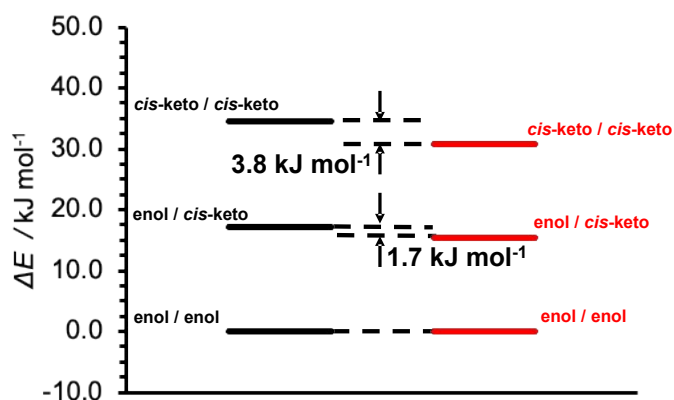


Figure S19 Energy diagram for the tautomers that compares the isolation model (black bars) and cluster model (red bars).

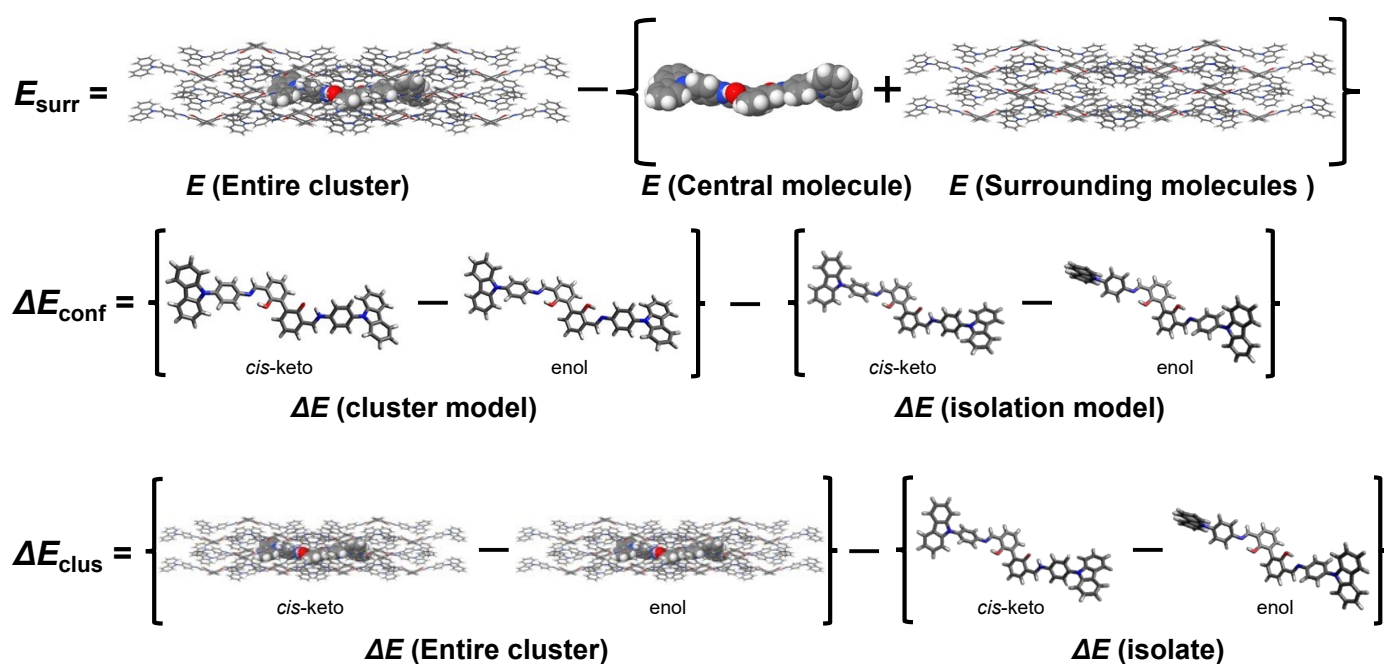


Figure S20 Scheme for calculating E_{surr} , ΔE_{conf} and ΔE_{clus} value.

Table S4 Various energies of tautomers derived from the cluster model calculations.^{a)} The ΔE values are shown as referenced by the energy of enol/enol form.

	$\Delta E_{\text{surr}}^a / \text{kJ mol}^{-1}$	$\Delta E_{\text{conf}} / \text{kJ mol}^{-1}$	$\Delta E_{\text{clus}} / \text{kJ mol}^{-1}$
enol / enol	(0.0)	(0.0)	(0.0)
enol / <i>cis</i> -keto	-13.2	-1.7	-15.0
<i>cis</i> -keto / <i>cis</i> -keto	-25.0	-3.8	-28.8

a) See definition in Fig. S18

Table S5 Energy values^{a)} per molecule ($E / \text{kJ mol}^{-1}$) of the **bis-SACz** cluster at each step in the iterative optimization. Difference from the previous step is given in parentheses.

	@2→@3	@3→@4	@4→@5	@5→@6
High real	(0)	-0.7681	-0.0651	-0.6339
High model	(0)	0.0236	0.0230	0.0224
Low model	(0)	0.0206	0.0428	0.0181
Low real	(0)	-0.7712	-0.0453	-0.6383

a) ONIOM(B3LYP/6-311G**:*HF*/STO-3G) Opt

Table S6 The RMS values of the atomic displacement (\AA) of heavy atoms from initial structure during iterative optimization of the cluster model calculation. For detail, see main text.

	@1	@2	@3	@4	@5
RMS	0.07889	0.07926	0.06516	0.07108	0.06559
Standard error	0.00141	0.00142	0.00116	0.00127	0.00117

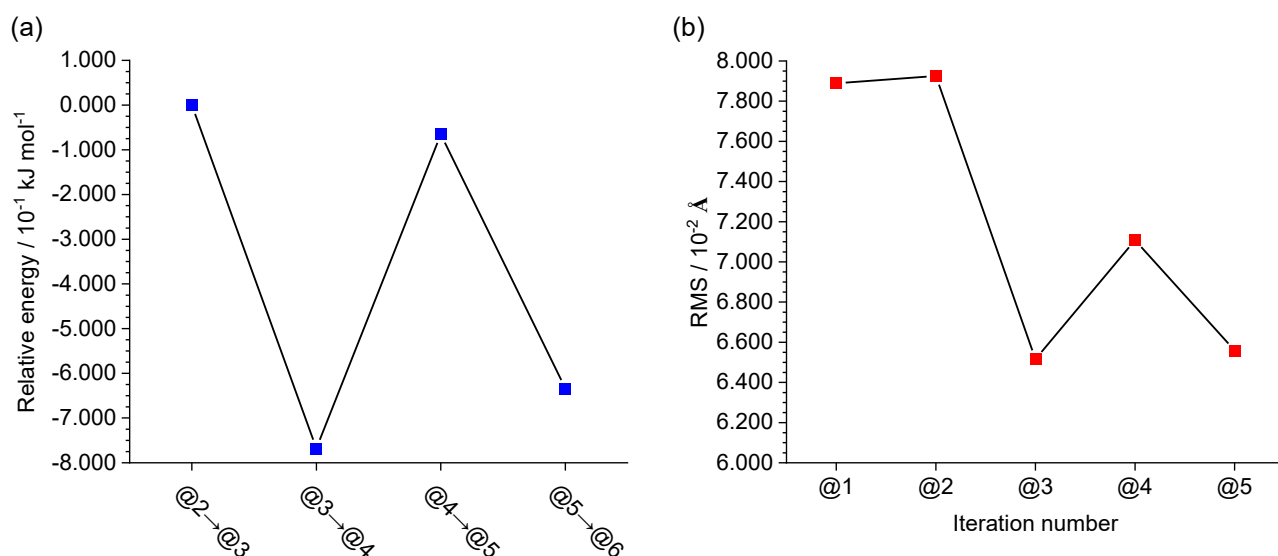


Figure S21 (a) Energy and (b) RMS values of the cluster model of **bis-SACz** as functions of the iteration step of optimization.

Table S7 Relative energy between tautomers of **bis-SACz** cluster model as a function of the iteration step of optimization. The ΔE values^{a)} are shown as referenced by the energy of enol/enol form.

	High real	high model	low model	low real
@2	$\Delta E / \text{kJ mol}^{-1}$			
enol/enol	(0)	(0)	(0)	(0)
enol/ <i>cis</i> -keto	1.79	14.51	10.57	-2.15
<i>cis</i> -keto / <i>cis</i> -keto	5.38	29.76	23.24	-1.14
@3				
enol/enol	(0)	(0)	(0)	(0)
enol/ <i>cis</i> -keto	2.25	15.50	12.08	-1.16
<i>cis</i> -keto / <i>cis</i> -keto	5.71	30.73	24.82	-0.20
@4				
enol/enol	(0)	(0)	(0)	(0)
enol/ <i>cis</i> -keto	2.15	15.00	11.10	-1.75
<i>cis</i> -keto / <i>cis</i> -keto	5.65	30.25	23.84	-0.77
@5				
enol/enol	(0)	(0)	(0)	(0)
enol/ <i>cis</i> -keto	2.56	15.20	11.91	-0.73
<i>cis</i> -keto / <i>cis</i> -keto	6.10	30.48	24.70	0.32

a) ONIOM (B3LYP/6-311G** : HF/6-31G)

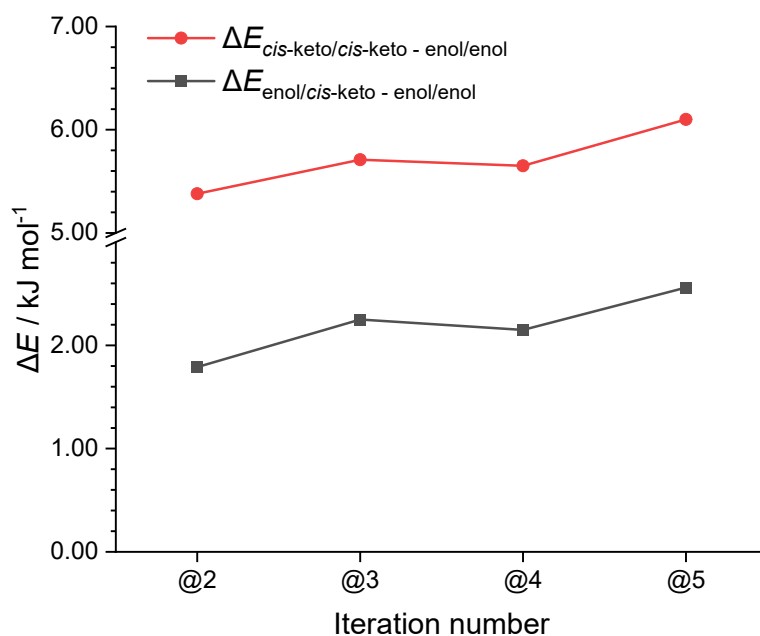


Figure S22 Relative energy between tautomers of **bis-SACz** cluster model as a function of the iteration step of optimization.

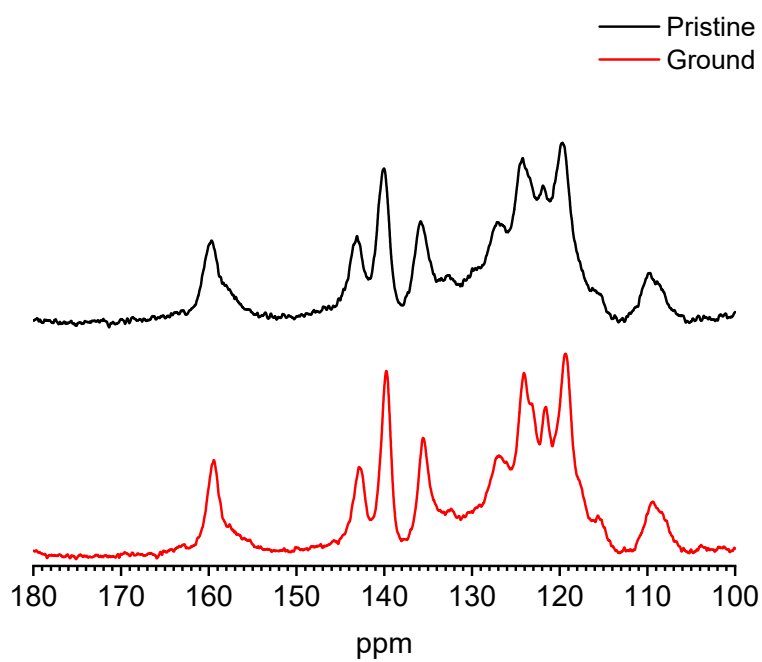


Figure S23 Solid-state CP-MAS ^{13}C NMR spectra of pristine (black line) and ground (red line) **bis-SACz**.

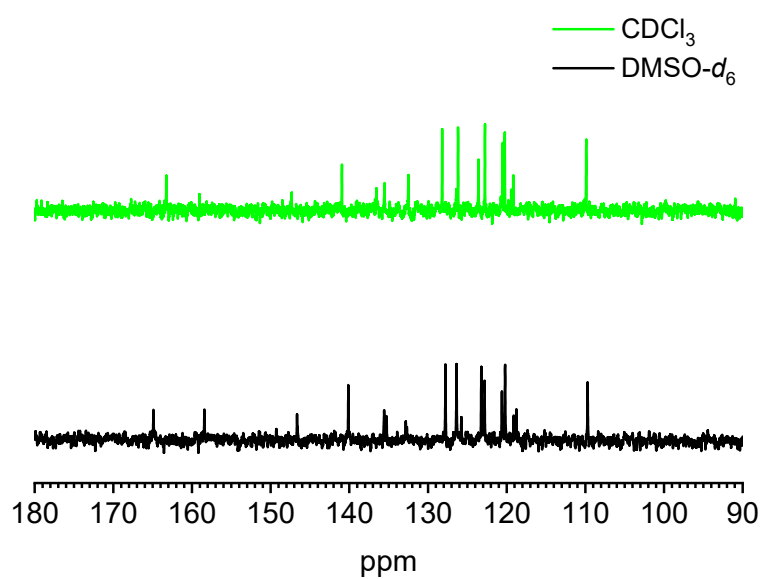


Figure S24 ^{13}C NMR (100 MHz) spectra of **bis-SACz** measured for CDCl_3 (green line) and $\text{DMSO-}d_6$ (black line) solutions.

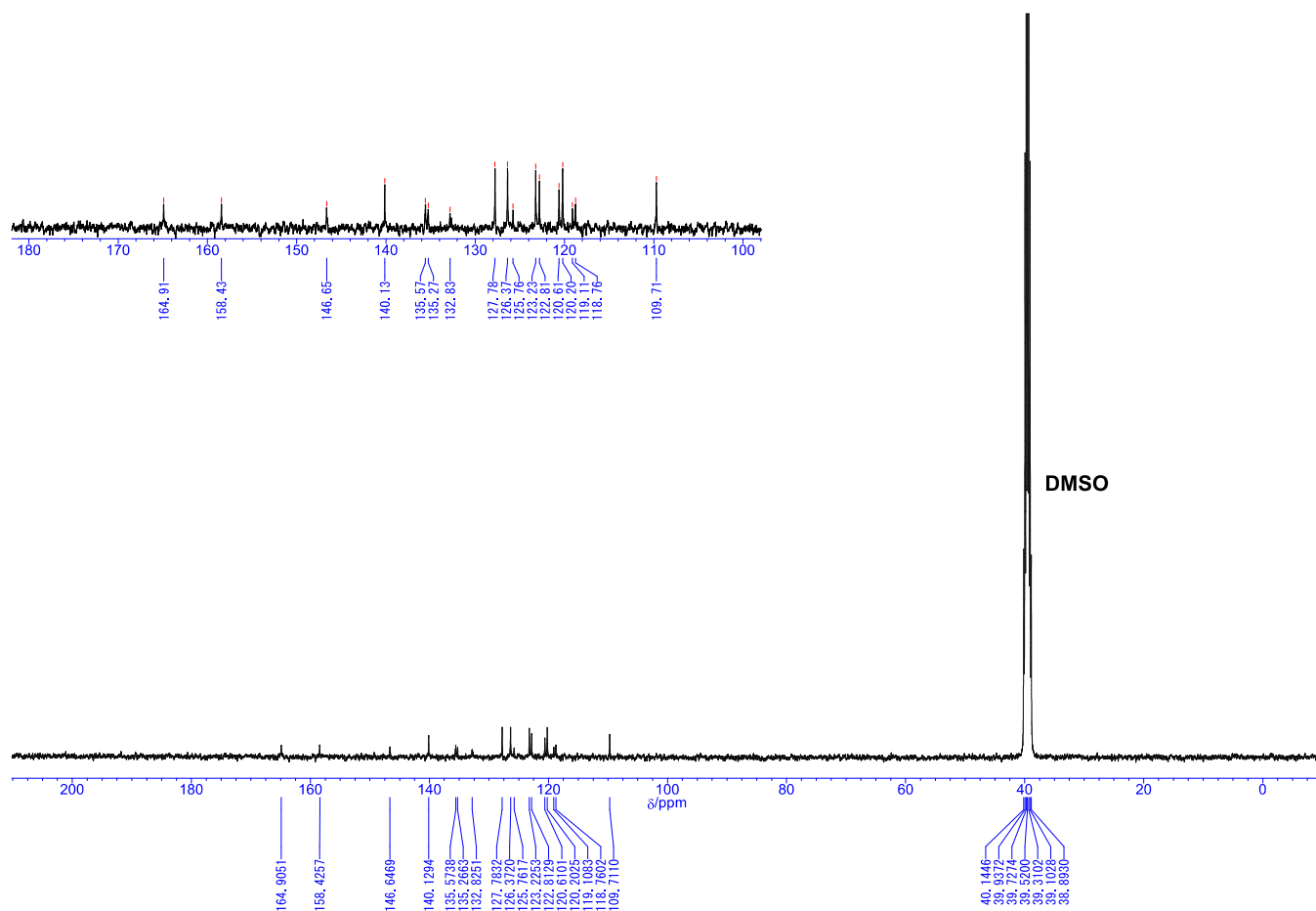


Figure S25 ^{13}C NMR (100 MHz, $\text{DMSO-}d_6$) spectra of compound bis-SACz.

References

- (1) G. M. Sheldrick, *Acta Crystallogr., Sect. A: Found.* **2008**, *64*, 112.
- (2) G. M. Sheldrick, *Acta Crystallogr., Sect. C: Struct. Chem.* **2015**, *71*, 3.
- (3) C. Kabuto, S. Akine, T. Nemoto and E. Kwon, *Nihon Kessho Gakkaishi* **2009**, *51*, 218.
- (4) M. I. Mangione, R. A. Spanevello and M. B. Anzardi, *RSC Adv.*, **2017**, *7*, 47681
- (5) A. Kundu, S. Karthikeyan, D. Moon and S. P. Anthony, *ChemistrySelect*, **2018**, *3*, 7340–7345.
- (6) S. Wünnemann, R. Fröhlich and D. Hoppe, *European J. Org. Chem.*, **2008**, 2008, 684–692.